On the Decoding Performance of Spatially Coupled LDPC Codes with Sub-block Access

Eshed Ram Yuval Cassuto
Andrew and Erna Viterbi Department of Electrical and Computer Engineering
Technion – Israel Institute of Technology, Haifa 32000, Israel
E-mails: {s6eshedr@, ycassuto@ee}.technion.ac.il

***Abstract*—We study spatially coupled LDPC codes that allow access to sub-blocks much smaller than the full code block. Sub-block access is realized by a semi-global decoder that decodes a chosen target sub-block by only accessing the target, plus a prescribed number of helper sub-blocks adjacent in the code chain. This paper analyzes the semi-global decoding performance of spatially coupled LDPC codes constructed from protographs. The main result shows that semi-global decoding thresholds can be derived from certain thresholds we define for the single-sub-block graph. These characterizing thresholds are also used for deriving lower bounds on the decoder's performance over channels with variability and memory across sub-blocks, which are motivated by applications in data storage.**

I. Introduction

Spatially coupled low-density parity-check (SC-LDPC) codes [1] have been shown to be an attractive class of graph codes, thanks to their good performance in both asymptotic and finite-block regimes. Most of their good properties stem from the convolution-like structure imposed on their code graphs. A very popular and effective construction method for SC-LDPC codes uses chaining of coupled protographs [2], where extremely simple protographs (e.g. regular) are often sufficient for extremely good performance [3], [4]. Another advantage of the convolutional structure lies in its enabling of efficient low-latency decoders such as the window decoder [5], [6]. SC-LDPC codes have been the subject of very active research recently (see e.g. [7], [8], [9], [10], [11]), improving their performance in different scenarios. In this paper, we harness the convolutional structure of SC-LDPC codes toward a new feature: allowing selective decoding of target sub-blocks within the full code block, without requiring to start the decoding from the beginning of the block. This feature is attractive for deploying SC-LDPC codes in storage applications, which require read access to small units of data at low latency.

In a recent series of papers [12], [13], [14], [15], a new type of SC-LDPC codes for efficient sub-block access is presented and studied. These codes, called SC-LDPCL codes (suffix 'L' stands for locality), can be decoded locally at the level of sub-blocks that are much smaller than the full code block, thus offering fast access to the coded information alongside the strong reliability of the global full-block decoding. Earlier work on codes with sub-block access includes multi-sub-block Reed-Solomon codes in [16], and multi-sub-block LDPC codes (without spatial coupling) in [17].

This paper contributes a theoretical methodology for analyzing the performance of a general class of SC-LDPCL codes decoded by the *semi-global (SG) decoder*, first defined in [12]. SG decoding is an intermediate decoding mode in between local and global decoding, in which a prescribed number d of *helper* sub-blocks can be accessed in addition to a *target* sub-block requested by the user. In Section III, we detail an efficient method to determine or bound the *SG decoding thresholds* (in the limit of large d), for both cases of starting from a termination or non-termination sub-block. The key component of this method (Section III-A), is a characterization of certain thresholds for the *single sub-block code* that are shown to govern the performance of the SG decoder accessing an arbitrary number of sub-blocks. The link between the single sub-block thresholds and SG decoding performance is established by a density-evolution analysis formalizing and accounting for the information transfer between subsequent sub-blocks in the decoding process. In Section IV, we study the performance of SG decoding over channels with variability and memory, motivated by applications in which the channel quality varies across information sub-units (e.g., pages in data storage [18], [19]), and with proximate sub-units having correlated quality parameters.

This paper extends the prior results of [12] on SC-LDPCL codes in several ways: 1) it introduces a new analysis method based on single-sub-block thresholds, and as a result, 2) it enables the construction of general unit-memory codes instead of only cutting-vector based as in [12]. In addition, 3) it extends the analysis on channels with sub-block variability from an i.i.d. model to a Markov model with spatial memory. For simplicity and clarity, we present the results assuming density evolution over the binary erasure channel (BEC), but the results can be extended to other channels using known extensions of the density-evolution method [20], [21]. Due to space limit, key results are given without proofs. The full proofs can be found in [22].

II. SC-LDPC and SC-LDPCL Background

An LDPC protograph [2] is a bipartite graph represented via a bi-adjacency matrix B (a protomatrix). The protograph is used as a base graph to construct a Tanner graph. We focus here on asymptotic performance, hence we skip the details

This work was supported in part by the Israel Science Foundation and in part by the US-Israel Binational Science Foundation.

of the lifting operation performed for obtaining a long code from B (see [3]). We analyze the protographs over the binary erasure channel BEC(ϵ), and write $\epsilon^*(B)$ for the belief-propagation (BP) decoding threshold of the protograph B.

An (l,r)-regular SC-LDPC protograph[1] is constructed as follows. Let $B = 1^{l\times r}$ be an all-ones base matrix, let $T \geq 1$ be an integer *memory* parameter, and let $\{B_\tau\}_{\tau=0}^{T}$ be binary matrices such that $B = \sum_{\tau=0}^{T} B_\tau$ (in this paper we consider only binary B matrices). Coupling $M > 1$ copies of B amounts to diagonally placing M copies of $\left(B_0; B_1; \cdots; B_T\right)$ in the coupled matrix (for more details, see [3]). Throughout this paper, we consider (l,r)-regular SC-LDPC protographs with memory $T=1$, i.e., $B = 1^{l\times r}$ and $B_1 = 1^{l\times r} - B_0$. We call such codes *unit-memory binary-regular SC-LDPC codes*. The results can be extended to higher-memory codes with some technical modifications. For example, using higher memory will add connectivity in the SC code which can be helpful in terms of SG decoding over channels with memory.

A. SC-LDPCL: Codes With Sub-Block Locality

To endow SC-LDPC codes with more flexible access, we divide the codeword to M sub-blocks (SBs), where each SB corresponds to one copy of $(B_0;B_1)$ in the coupled matrix. We define an (l,r,t)-regular SC-LDPC code with SB locality (in short SC-LDPCL) to be an (l,r)-regular SC-LDPC protograph with a partitioning that is constrained such that B_0 has $l-t \geq 2$ all-one rows and t mixed rows (i.e., with ones and zeros). The all-one and mixed rows correspond to *local checks* (LC) and *coupling checks* (CC), respectively (LCs are connected to only within SBs, and CCs connect between SBs). The resulting protograph can be visualized as a chain of $M > 1$ coupled SBs, where each SB is an $(l-t,r)$-regular local code, and adjacent SBs are connected via t coupling checks with connections specified by the t mixed rows in B_0.

Let B_{loc} be the $(l-t)\times r$ all-ones matrix that forms the *local* part of B_0, and let $B_{\text{left}}, B_{\text{right}}$ be the $t\times r$ matrices that form the *coupling* parts of B_0, B_1, respectively. Then, the coupled protomatrix can be written as

$$\begin{pmatrix} \ddots & B_{\text{loc}} & & & \\ & B_{\text{right}} & B_{\text{left}} & & \\ & & B_{\text{loc}} & & \\ & & B_{\text{right}} & B_{\text{left}} & \\ & & & B_{\text{loc}} & \ddots \end{pmatrix}. \tag{1}$$

B_{left} and B_{right} connect a SB to its neighbors on the left and right, respectively.

Example 1. *For $l=3, r=6, t=1$, the specific SC-LDPCL construction proposed in [13] yields*

$$\left(\begin{array}{c} B_{\text{left}} \\ \hline B_{\text{loc}} \\ \hline B_{\text{right}} \end{array}\right) = \left(\begin{array}{cccccc} 1&1&1&0&0&0 \\ \hline 1&1&1&1&1&1 \\ 1&1&1&1&1&1 \\ \hline 0&0&0&1&1&1 \end{array}\right). \tag{2}$$

[1]The term regular refers to the protomatrix B, while the resulting coupled graph is not regular due to termination.

B. Semi-Global Decoding

In SG decoding [12], the user is interested in SB $m \in \{1,\ldots,M\}$, which is called the *target* SB, and the decoder decodes it with the help of additional d neighbor SBs called *helper* SBs. In SG decoding there are two phases: the *helper phase*, and the *target phase*. In the former, helper SBs are decoded locally, incorporating information from other previously decoded helper SBs. In the latter, the target SB is decoded while incorporating information from its neighboring helper SBs.

III. Threshold Analysis of SG Decoding

We now detail the theoretical threshold analysis for SG decoding of SC-LDPCL protographs defined in Section II-A. Our key analysis tool is a family of decoding thresholds that can be efficiently computed from the protomatrix *of a single SB*, and in turn be used to derive the performance of the SG decoder spanning an arbitrary number of SBs.

A. Single-SB Thresholds

The proposed thresholds are defined over *erasure-transfer functions*, defined next.

Definition 1. *Consider a helper SB during SG decoding. Let $\epsilon \in [0,1]$ be the SB's erasure rate, and let $\underline{\delta}_I \in [0,1]^t$ be the incoming DE values from a previously decoded helper. The **erasure-transfer function** outputs $\underline{\delta}_O \in [0,1]^t$, given the input arguments ϵ and $\underline{\delta}_I$. We denote by $\Delta_L(\epsilon, \underline{\delta}_I)$ and $\Delta_R(\epsilon, \underline{\delta}_I)$ the erasure-transfer functions corresponding to right and left helper SBs, respectively.*

When considering an erasure-transfer function $\Delta(\epsilon, \underline{\delta})$ (right or left), we identify three important channel-parameter thresholds[2] $\epsilon_1^*, \epsilon_2^*, \epsilon_3^*$. We call them the *single-SB thresholds*. The first threshold ϵ_1^* is the largest channel parameter that gives all-0 erasure-transfer output for any $\underline{\delta}_I$:

$$\Delta(\epsilon, \underline{\delta}) = \underline{0}, \quad \forall \epsilon < \epsilon_1^*, \quad \forall \underline{\delta} \in [0,1]^t. \tag{3}$$

In [22] it is shown that ϵ_1^* is the threshold induced by the protograph B_{loc}. The second threshold ϵ_2^* is the largest channel parameter such that

$$\Delta(\epsilon, \underline{\delta}) \prec \underline{\delta}, \quad \forall \epsilon < \epsilon_2^*, \quad \forall \underline{\delta} \in [0,1]^t. \tag{4}$$

Practically, this means that sufficiently many consecutive helpers with $\epsilon < \epsilon_2^*$ will decrease the transferred erasure rate to zero. We calculate ϵ_2^* by computing $\Delta(\epsilon, \underline{\delta})$ for all $\underline{\delta} \in [0,1]^t$ (sampled on a grid) and with increasing values of ϵ until (4) is violated. The third threshold ϵ_3^* is the largest channel parameter such that incoming all-0 DE values are preserved in the output, i.e.,

$$\Delta(\epsilon, \underline{0}) = \underline{0}, \quad \forall \epsilon < \epsilon_3^*. \tag{5}$$

In addition, we define $\epsilon_{l,r}^*$ to be the threshold of the regular (l,r) (block-LDPC) ensemble.

[2]These thresholds are properties of the protograph used, however, for ease of reading we make this implicit in the notations.

Example 2. *Consider the $(l=3, r=6, t=1)$ SC-LDPCL protograph from Example 1*[3]. *The SB thresholds of this protograph are given by $\epsilon_1^*=0.2, \epsilon_2^*=0.3719, \epsilon_3^*=0.4297$. In addition, $\epsilon_{l,r}^*=0.4294$.*

Finally, we define the two-sided threshold $\epsilon^*(\underline{\delta}_L, \underline{\delta}_R)$ as the maximum erasure rate such that the SB is successfully decoded *locally* given incoming DE values $\underline{\delta}_L$ from left and $\underline{\delta}_R$ from right. For example, if $\underline{\delta}_L = \underline{\delta}_R = \underline{1}$, then the SB cannot use any side information, and its threshold is the local threshold, i.e., $\epsilon^*(\underline{1}, \underline{1}) = \epsilon_1^*$. Furthermore, we have the following result (proof omitted).

Proposition 1. *For left and right helper SBs, $\epsilon^*(\underline{0}, \underline{1}) = \epsilon_3^* = \epsilon^*([B_{left}; B_{loc}])$, and $\epsilon^*(\underline{1}, \underline{0}) = \epsilon_3^* = \epsilon^*([B_{loc}; B_{right}])$, respectively.*

B. SG Decoding Thresholds over Memoryless Channels

We now derive the thresholds for SG decoding in the limit of large d, when decoding starts from a termination or non-termination SBs. Toward this end, we use a binary parameter $\tau \in \{0,1\}$ to mark the first-accessed-helper type: termination ($\tau = 0$) or non-termination ($\tau = 1$). The results in this section apply to unit-memory binary-regular SC-LDPC codes, but for terseness we keep this implicit in most of the result statements. The thresholds are now defined.

Definition 2. *Let $\tau_L, \tau_R \in \{0,1\}$ indicate termination SBs ($\tau = 0$) or not ($\tau = 1$) from left and right of the target SB, respectively. We define $\epsilon_{SG}^{\tau_L;\tau_R}$ as the largest channel parameter such that the SG decoder successfully decodes the target SB in the limit of $d \to \infty$ helper SBs.*

For simplicity of the derivations, we assume that the SBs are symmetric ($\Delta_L = \Delta_R \triangleq \Delta$). For $\tau \in \{0,1\}$, let $\underline{\delta}_0^{(\tau)}(\epsilon), \underline{\delta}_1^{(\tau)}(\epsilon), \ldots$ be the sequence of inter-SB DE values between helper SBs during SG decoding, with $\tau = 0$ if decoding starts in a termination SB, and $\tau = 1$ otherwise,

$$\begin{aligned} &\underline{\delta}_{i+1}^{(\tau)}(\epsilon) = \Delta\left(\epsilon, \underline{\delta}_i^{(\tau)}\right), \quad i \geq 0, \, \tau \in \{0,1\}, \\ &\underline{\delta}_0^{(0)} = \underline{0}, \quad \underline{\delta}_0^{(1)} = \underline{1}. \end{aligned} \tag{6}$$

For every ϵ, $\Delta(\epsilon, \underline{\delta})$ is monotonically non-decreasing[4] in $\underline{\delta}$. Consequently, for $\tau \in \{0,1\}$ the sequences $\{\underline{\delta}_i^{(\tau)}(\epsilon)\}_{i \geq 0}$ (which are bounded by $[0,1]$) converge to some limit value.

Definition 3. *For $\tau \in \{0,1\}$, let $\hat{\underline{\delta}}^{(\tau)}(\epsilon) = \lim_{i\to\infty} \underline{\delta}_i^{(\tau)}(\epsilon)$.*

In view of (6) and Definition 3, for every $\epsilon \in [0,1]$, $\Delta\left(\epsilon, \hat{\underline{\delta}}^{(\tau)}(\epsilon)\right) = \hat{\underline{\delta}}^{(\tau)}(\epsilon)$.

From the fact that termination can only help and from symmetry, we know that $\epsilon_{SG}^{1,1} \leq \epsilon_{SG}^{0,1} = \epsilon_{SG}^{1,0} \leq \epsilon_{SG}^{0,0}$. We now provide results we can prove on the different SG thresholds (proofs omitted).

[3]This protograph has a symmetry property that gives $\Delta_L(\cdot,\cdot) = \Delta_R(\cdot,\cdot)$, thus we denote both erasure-transfer functions as $\Delta(\cdot,\cdot)$. Note that for $t=1$, the input δ_I and output δ_O of $\Delta(\cdot,\cdot)$ are scalars.

[4]Please do not confuse this property with the fact that $\Delta(\epsilon, \underline{\delta})$ may be smaller or larger than $\underline{\delta}$.

Proposition 2. *$\epsilon_{SG}^{1,1} \geq \epsilon_2^*$, where ϵ_2^* is given in (4).*

Proposition 3. *$\epsilon_{SG}^{0,0} \leq \epsilon^*(\underline{0}, \underline{0})$, where $\epsilon^*(\cdot,\cdot)$ is defined in Section III-A*

Theorem 4. *$\epsilon_{SG}^{0,1} \geq \epsilon_3^*$. In addition, if $\epsilon_{l,r}^* \leq \epsilon_3^*$ and for every $\epsilon > \epsilon_3^*$, $\hat{\underline{\delta}}^{(0)}(\epsilon) = \hat{\underline{\delta}}^{(1)}(\epsilon)$, then $\epsilon_{SG}^{0,0} = \epsilon_{SG}^{0,1} = \epsilon_3^*$.*

Remark 1. *The conditions $\epsilon_{l,r}^* \leq \epsilon_3^*$ and $\hat{\underline{\delta}}^{(0)}(\epsilon) = \hat{\underline{\delta}}^{(1)}(\epsilon)$ for $\epsilon > \epsilon_3^*$ hold for many constructions (see Example 2). $\epsilon_{l,r}^*$ is the threshold of the $l \times r$ all-ones matrix, while in view of Proposition 1, for left helper SBs, ϵ_3^* equals to the threshold of the $l \times r$ protomatrix $[B_{left}; B_{loc}]$. For many assignments of B_{left}, we will get $\epsilon_{l,r}^* \leq \epsilon_3^*$ (see Table I in Section IV-D). In addition, the condition $\hat{\underline{\delta}}^{(0)}(\epsilon) = \hat{\underline{\delta}}^{(1)}(\epsilon)$ holds whenever $\Delta(\epsilon, \underline{\delta}) = \underline{\delta}$ for a unique $\underline{\delta} \in [0,1]^t$. In all of the DE enumerations that we have done, this was the case.*

The meaning of $\epsilon_{SG}^{0,0} = \epsilon_{SG}^{0,1}$ in Theorem 4 is that for constructions that satisfy the added conditions in Theorem 4, if one side starts from a termination, it does not help to start the other side from termination.

IV. Performance Over The Sub-Block Markov-Varying (SBMV) Channel

We now turn to analyze SC-LDPCL codes over channels with SB-variability and memory. SG decoding is especially attractive for channels with variability, thanks to the opportunity to have high-quality helper SBs contributing sufficient information toward successful target decoding. We model the channel as a *Markov chain* (Section IV-A), and for the analysis we define another: a simplified channel Markov chain to fit the SB thresholds of the code ensemble (Section IV-B).

A. SBMV Channel Model

Let $\mathcal{E} = \{e_1, e_2, \ldots, e_{|\mathcal{E}|}\}$ be the possible channel states (erasure rates), and let $\{E_m\}_{m=1}^M$ be a Markov chain describing the channel state of SBs $m \in \{1, 2, \ldots, M\}$, with the transition probabilities

$$\Pr\left(E_m = e_j \middle| E_{m-1} = e_i\right) = P_{i,j}, \quad \forall\, 2 \leq m \leq M, \tag{7}$$

where P is a given $|\mathcal{E}| \times |\mathcal{E}|$ transition matrix. We make all the standard assumptions about the Markov chain, in particular having a unique stationary distribution $\underline{\nu} = (\nu_1, \nu_2, \ldots, \nu_{|\mathcal{E}|})$, such that the *expected erasure rate* of the SBMV channel is $\mathbb{E}[E_m] = \sum_{i=1}^{|\mathcal{E}|} \nu_i e_i$.

B. Code Ensemble's Sub-Block States

From the perspective of the chosen code ensemble, the SB states are the projection of the channel states (from Section IV-A) on the thresholds defined in (3)–(5). Accordingly, we define the following four states. s_1 (local decoding interval): when the channel parameter is in $[0, \epsilon_1^*)$, that is, the SB is decodable locally; s_2 (error-reduction interval): for parameters in $[\epsilon_1^*, \epsilon_2^*)$, where the inter-DE values between SBs decrease; s_3 (error-free-preservation interval): parameters in $[\epsilon_2^*, \epsilon_3^*)$, where all-0 incoming DE values are preserved; and s_4 (anti-termination interval): in $[\epsilon_3^*, 1]$, where the outgoing DE values are arbitrarily high, regardless of the incoming DE values. Let $\{B_m\}_{m=1}^{M}$ be a Markov chain describing the state of SBs $m \in \{1, 2, \ldots, M\}$ with a state space $\mathcal{S} = \{s_1, s_2, s_3, s_4\}$. The following results tie the chain $\{B_m\}_{m=1}^{M}$ to the channel chain $\{E_m\}_{m=1}^{M}$ defined in Section IV-A. For every $i \in \{1, 2, 3, 4\}$, let $\mu_i \triangleq \sum_{k \in s_i} \nu_k$. Then the transition probabilities of $\{B_m\}_{m=1}^{M}$ can be written as $Q_{i,j} = \frac{1}{\mu_i} \sum_{i' \in s_i} \sum_{j' \in s_j} \nu_{i'} P_{i',j'}$. Moreover, the stationary distribution of $\{B_m\}_{m=1}^{M}$ is given by $\underline{\mu} = (\mu_1, \mu_2, \mu_3, \mu_4)$.

In view of the strict monotonicity prescribed in (4), for every $\epsilon < \epsilon_2^*$, we define

$$q(\epsilon) = \min\{k \in \mathbb{N} \colon \Delta^{(k)}(\epsilon, \underline{1}) = \underline{0}\}, \tag{8}$$

where $\Delta^{(k)}$ denotes the k-th sequential invocation of Δ with $\underline{\delta}_O$ of the i-th invocation used as $\underline{\delta}_I$ of the $i+1$-st. $q(\epsilon)$ in (8) is the minimum number of subsequent sub-blocks needed to drive the inter-sub-block DE values from $\underline{1}$ (no information) to $\underline{0}$ (full information). Finally, define the $(q+2) \times (q+2)$ matrix

$$Q_q = \left(\begin{array}{c|c|c|c|c} 1 & 0 & 0 & 0 & 0 \\ \hline Q_{2,1} & 0 & Q_{2,2} \cdot I_{q-2} & Q_{2,3} & Q_{2,4} \\ \hline Q_{2,1} + Q_{2,2} & 0 & 0 & Q_{2,3} & Q_{2,4} \\ \hline Q_{3,1} & Q_{3,2} & 0 & Q_{3,3} & Q_{3,4} \\ \hline 0 & 0 & 0 & 0 & 1 \end{array}\right). \tag{9}$$

C. SG Decoding Performance

We now state lower bounds on the probability of SG-decoding success over the SBMV channel. We state the main result of this section omitting the proof from [22], which interestingly uses a third Markov chain tracking the state of the decoder.

Proposition 5. *Let e be the maximal value in $\mathcal{E}$ in the interval $[\epsilon_1^*, \epsilon_2^*)$, and let $q = q(e)$ according to (8) ($q = 0$ if no e is in this interval). The success probability of SG-decoding with parameter d (even), over the SBMV channel P is lower bounded by $p(d) \geq \underline{v}\left(Q_q^{d/2} \otimes \hat{Q}_q^{d/2}\right)\underline{u}^T$, where Q_q is defined in (9), $\hat{Q}_q$ is constructed as in (9) with the substitution $\hat{Q}_{i,j} = \frac{\mu_j}{\mu_i} Q_{j,i}$, $\otimes$ is the Kronecker product, and $\underline{v} = (v_1, \ldots, v_{(q+2)^2})$, $\underline{u} = (u_1, \ldots, u_{(q+2)^2})$ are given by*

$$v_{j+(q+2)(i-1)} = \begin{cases} \mu_1 & j = i = 1 \\ \mu_2 & j = i = 2 \\ \mu_3 & j = i = q+1 \\ \mu_4 & j = i = q+2 \\ 0 & \textit{otherwise} \end{cases}, \qquad 1 \leq i, j \leq q+2.$$

$$u_{j+(q+2)(i-1)} = \begin{cases} 1 & i = 1 \textit{ or } j = 1 \\ 0 & \textit{otherwise} \end{cases}$$

Example 3. *Consider the SBMV channel with $\mathcal{E} = \{e_1 = 0.175, e_2 = 0.35, e_3 = 0.42, e_4 = 0.47\}$, and*

$$P_1 = \begin{pmatrix} 0 & 0.5 & 0.5 & 0 \\ \beta & \alpha & 1-\alpha-2\beta & \beta \\ \beta & 1-\alpha-2\beta & \alpha & \beta \\ 0 & 0.5 & 0.5 & 0 \end{pmatrix} \tag{10}$$

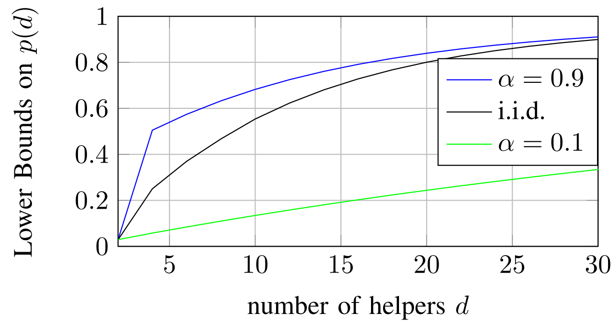

Fig. 1. Plots corresponding to Proposition 5 for the SBMV channel P_1 with two α values, and the i.i.d. channel with the same average quality.

for some parameters $0 < \alpha, \beta < 1$ such that $\alpha + 2\beta \leq 1$. We use the $(l = 3, r = 6, t = 1)$ SC-LDPCL protograph from Example 1, whose thresholds imply that for every $i \in \{1, 2, 3, 4\}$, $s_i = \{i\}$, and $q = q(e_2) = 3$. We set $\beta = 0.01$ in P_1, yielding for every $0 \leq \alpha \leq 0.98$ the stationary distribution $(0.0098, 0.4902, 0.4902, 0.0098)$, and compare in Figure 1 this channel with two choices of α and an i.i.d. channel with the same expected erasure rate. The $\alpha = 0.9$ channel, which has positive correlation between neighboring SBs, shows (in blue) better performance than the i.i.d. model (black), and a larger advantage over the $\alpha = 0.1$ channel model (green), for all d.

D. Code Design

We now perform a threshold analysis and performance evaluation of SG decoding for a family of SC-LDPCL protographs sharing the same code rate and node degrees, however, differing in edge spreading. We focus on protographs that have left/right symmetry, and consider coupling parameters $t \leq 2$. Let $l = 4$ and $r = 6$ be the column and row weight of the underlying base matrix B. We consider $t \in \{0, 1, 2\}$ ($t = 0$ corresponds to an isolated SB, and $t \in \{1, 2\}$ corresponds to a SB in a proper SC-LDPC code).

In the case of $t = 0$, each SB is an (l, r) code. Since there are no coupling checks, all of the SBs' thresholds coincide $\epsilon_3^* = \epsilon_2^* = \epsilon_1^* = 0.5061$. For $t = 1$, we have only a single edge-spreading rule that induces symmetric SBs. In this protograph $B_{\text{left}} = \begin{pmatrix} 1 & 1 & 1 & 0 & 0 & 0 \end{pmatrix}$. The SB thresholds for the $t = 1$ code are $\epsilon_1^* = 0.4294$, $\epsilon_2^* = 0.4788$, $\epsilon_3^* = 0.5474$. If we use $t = 2$ coupling check nodes, then more edge-spreading rules are possible. We calculated the SB thresholds for all of the possible edge-spreading rules for $t = 2$ and found (see details in [22]) that there is one code that dominates all others, in terms of SG-decoding performance. This code is given by

$$B_{\text{left}} = \begin{pmatrix} 1 & 1 & 0 & 0 & 0 & 0 \\ 0 & 1 & 1 & 1 & 1 & 0 \end{pmatrix}. \tag{11}$$

The local threshold is $\epsilon_1^* = 0.2$; the other thresholds, alongside with the q value (see (8)) for erasure parameter 0.435, are given in Table I for all of the considered codes (i.e., $t = 0, 1, 2$). Also shown are the global thresholds ϵ_G^*: the threshold of the coupled protograph [12] with $M = 50$ SBs.

TABLE I
THRESHOLDS OF $l = 4, r = 6$ (RATE 0.33) SC-LDPCL PROTOGRAPHS.

#	t	ϵ_1^*	ϵ_2^*	ϵ_3^*	ϵ_G^*	$q(0.435)$
1	0	0.5061	0.5061	0.5061	0.5061	1
2	1	0.4294	0.4788	0.5474	0.5564	2
3	2	0.2	0.4442	0.5722	0.5966	7

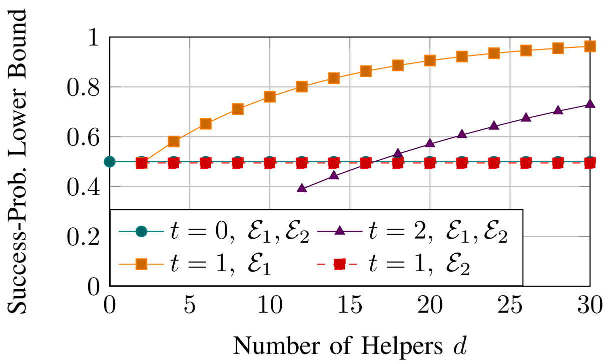

Fig. 2. Lower bounds on the success probabilities of SG decoding of three codes over two SBMV channels.

In what follows, we evaluate the SG performance of the above codes over the SBMV channel. We consider two channels, both with the transition matrix $P_2 = \begin{pmatrix}0.9\ 0.1; 0.1\ 0.9\end{pmatrix}$. For the first one, $\mathcal{E}_1 = \{0.435, 0.54\}$ and for the second, $\mathcal{E}_2 = \{0.435, 0.57\}$. Note that in some designs in Table I, the erasure rate in the "bad" state (0.54 and 0.57 for $\mathcal{E}_1$ and $\mathcal{E}_2$, respectively) is greater than ϵ_3^*. This means that in these particular cases, "bad" SBs are anti-termination SBs (i.e, in state s_4, see Section IV-B). For these cases, Proposition 5 simplifies to $p(d) = 0$ for $\frac{d}{2} < q - 1$ and $p(d) \geq 0.5 \cdot (2\alpha^{q-1} - \alpha^{2(q-1)})$, otherwise. Figure 2 shows the trade-offs between the different designs. The uncoupled protograph ($t = 0$) has the highest success probability for no helper SBs ($d = 0$), however, since the SBs are uncoupled, then adding helper SBs does not improve the performance. In addition, on one hand, the $t = 1$ design shows high success probabilities for the $\mathcal{E}_1$ channel, and on the other hand the performance is poor for the $\mathcal{E}_2$ channel. This degradation is a result of a relatively small ϵ_3^* threshold (0.5474, see line 2 in Table I). Furthermore, the $t = 2$ design shows the best performance for the $\mathcal{E}_2$ channel (for $d \geq 18$), while it requires high values for d (see $q = 7$ in Table I).

REFERENCES

[1] A. J. Felström and K. S. Zigangirov, "Time-varying periodic convolutional codes with low-density parity-check matrix," *IEEE Transactions on Information Theory*, vol. 45, no. 6, pp. 2181–2191, Sept. 1999.
[2] J. Thorpe, "Low-density parity-check (LDPC) codes constructed from protographs," 2003.
[3] D. G. M. Mitchell, M. Lentmaier, and D. J. Costello, "Spatially coupled LDPC codes constructed from protographs," *IEEE Transactions on Information Theory*, vol. 61, no. 9, pp. 4866–4889, 2015.
[4] D. G. M. Mitchell, L. Dolecek, and D. J. Costello, "Absorbing set characterization of array-based spatially coupled LDPC codes," in *2014 IEEE International Symposium on Information Theory*, Honolulu, HI, USA, 2014, pp. 886–890.
[5] A. R. Iyengar, R. L. U. P. H. Siegel, and J. K. Wolf, "Windowed decoding of spatially coupled codes," *IEEE Transactions on Information Theory*, vol. 59, no. 4, pp. 2277–2292, April 2013.
[6] M. Lentmaier, M. M. Prenda, and G. P. Fettweis, "Efficient message passing scheduling for terminated LDPC convolutional codes," in *2011 IEEE International Symposium on Information Theory (ISIT)*, St. Petersburg, Russia, Aug. 2011, pp. 1826–1830.
[7] H. Esfahanizadeh, A. Hareedy, and L. Dolecek, "Finite-length construction of high performance spatially-coupled codes via optimized partitioning and lifting," *IEEE Transactions on Communications*, vol. 67, no. 1, pp. 3–16, Jan. 2019.
[8] S. Mo, L. Chen, D. J. Costello, D. G. M. Mitchell, R. Smarandache, and J. Qiu, "Designing protograph-based quasi-cyclic spatially coupled LDPC codes with large girth," *IEEE Transactions on Communications*, vol. 68, no. 9, pp. 5326–5337, 2020.
[9] L. Tauz, H. Esfahanizadeh, and L. Dolecek, "Spatially coupled codes with sub-block locality: Joint finite length-asymptotic design approach," in *2020 IEEE International Symposium on Information Theory (ISIT)*, June. 2020, pp. 485–490.
[10] D. Truhachev, D. G. M. Mitchell, M. Lentmaier, D. J. Costello, and A. Karami, "Code design based on connecting spatially coupled graph chains," *IEEE Transactions on Information Theory*, vol. 65, no. 9, pp. 5604–5617, 2019.
[11] M. Zhu, D. G. M. Mitchell, M. Lentmaier, and D. J. Costello, "A novel design of spatially coupled LDPC codes for sliding window decoding," in *2020 IEEE International Symposium on Information Theory (ISIT)*, June. 2020, pp. 473–478.
[12] E. Ram and Y. Cassuto, "Spatially coupled LDPC codes with sub-block locality," *IEEE Transactions on Information Theory*, vol. 67, no. 5, pp. 2739–2757, 2021.
[13] E. Ram and Y. Cassuto, "Spatially coupled LDPC codes with random access," in *2018 IEEE 10th International Symposium on Turbo Codes Iterative Information Processing (ISTC)*, Hong-Kong, 2018, pp. 1–5.
[14] E. Ram and Y. Cassuto, "On decoding random-access SC-LDPC codes," in *2019 IEEE International Symposium on Information Theory (ISIT)*, Paris, France, 2019, pp. 2429–2433.
[15] H. Esfahanizadeh, E. Ram, Y. Cassuto, and L. Dolecek, "Spatially coupled codes with sub-block locality: Joint finite length-asymptotic design approach," in *2020 IEEE International Symposium on Information Theory (ISIT)*, June. 2020, pp. 467–472.
[16] Y. Cassuto, E. Hemo, S. Puchinger, and M. Bossert, "Multi-block interleaved codes for local and global read access," in *Proc. International Symposium on Information Theory (ISIT)*, Aachen, Germany, Jun. 2017, pp. 1758–1762.
[17] E. Ram and Y. Cassuto, "LDPC codes with local and global decoding," in *2018 IEEE International Symposium on Information Theory (ISIT)*, Vail, CO, USA, 2018, pp. 1151–1155.
[18] V. Taranalli, H. Uchikawa, and P. H. Siegel, "Channel models for multi-level cell flash memories based on empirical error analysis," *IEEE Transactions on Communications*, vol. 64, no. 8, pp. 3169–3181, 2016.
[19] E. Sharon, I. Alrod, R. Zamir, O. Fainzilber, I. Ilani, A. Bazarsky, and I. Goldenberg, "Low cost and power LDPC for commodity NAND products," in *The 11th Annual Non-Volatile Memories Workshop*. [Online]. Available: http://nvmw.ucsd.edu/nvmw2020-program/unzip/current2/nvmw2020-final29.pdf
[20] T. Richardson and R. Urbanke, *Modern Coding Theory*. USA: Cambridge University Press, 2008.
[21] G. Liva and M. Chiani, "Protograph LDPC codes design based on exit analysis," in *IEEE GLOBECOM 2007 - IEEE Global Telecommunications Conference*, Washington, DC, USA, 2007, pp. 3250–3254.
[22] E. Ram and Y. Cassuto, "On the decoding performance of spatially coupled LDPC codes with sub-block access," *Preprint*. [Online]. Available: https://arxiv.org/abs/2010.10616